Article

Cell Reports

Combined Loss of *Tet1* and *Tet2* Promotes B Cell, but Not Myeloid Malignancies, in Mice

Graphical Abstract

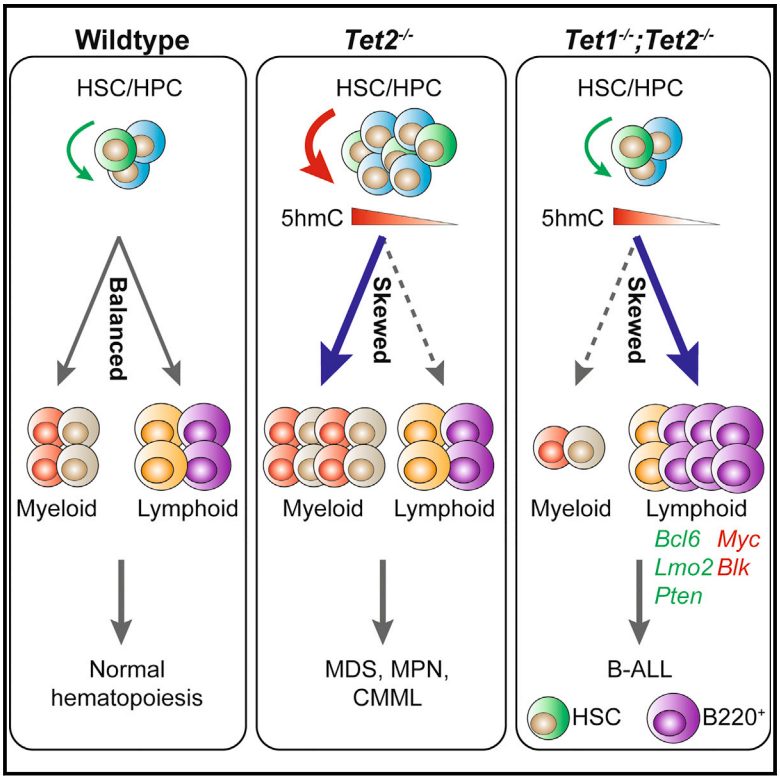

Highlights

- *TET1* and *TET2* are often concomitantly downregulated in acute B-lymphocytic leukemia
- Tet1 is required for *Tet2*-deletion-mediated HSC dysregulation and myeloid malignancy
- Deletion of both *Tet1* and *Tet2* in mice leads to lethal B cell malignancies
- *Tet2*$^{-/-}$ and *DKO* HSC/HPCs display distinct DNA 5hmC/5mC signatures

Authors

Zhigang Zhao, Li Chen, Meelad M. Dawlaty, ..., Rudolf Jaenisch, Peng Jin, Mingjiang Xu

Correspondence

jaenisch@wi.mit.edu (R.J.), peng.jin@emory.edu (P.J.), mxx51@miami.edu (M.X.)

In Brief

TET1 and TET2 are methylcytosine dioxygenases that are implicated in hematological malignancies. Using *Tet1* and *Tet2* double-knockout mice, Zhao et al. separate the roles of each enzyme and examine how Tet1 and Tet2 contribute to hematopoiesis and hematological malignancies.

Accession Numbers

GSE73611

Zhao et al., 2015, Cell Reports *13*, 1692–1704
November 24, 2015 ©2015 The Authors
http://dx.doi.org/10.1016/j.celrep.2015.10.037

OPEN ACCESS
CellPress

Cell Reports
Article

Combined Loss of *Tet1* and *Tet2* Promotes B Cell, but Not Myeloid Malignancies, in Mice

Zhigang Zhao,[1,2,3,10] Li Chen,[4,10] Meelad M. Dawlaty,[5,10] Feng Pan,[1,3,6] Ophelia Weeks,[6] Yuan Zhou,[7] Zeng Cao,[7] Hui Shi,[1,7] Jiapeng Wang,[3] Li Lin,[4] Shi Chen,[1] Weiping Yuan,[7] Zhaohui Qin,[8] Hongyu Ni,[9] Stephen D. Nimer,[1] Feng-Chun Yang,[1,3] Rudolf Jaenisch,[5,*] Peng Jin,[4,*] and Mingjiang Xu[1,3,*]

[1]Sylvester Comprehensive Cancer Center, Department of Biochemistry and Molecular Biology, University of Miami, Miami, FL 33136, USA
[2]Department of Hematology and Oncology, Tianjin Medical University Cancer Institute and Hospital, National Clinical Research Center for Cancer, Key Laboratory of Cancer Prevention and Therapy, Tianjin 300060, China
[3]Department of Pediatrics, Herman B. Wells Center for Pediatric Research, Indiana University School of Medicine, Indianapolis, IN 46202, USA
[4]Department of Human Genetics, Emory University School of Medicine, Atlanta, GA 30322, USA
[5]Whitehead Institute for Biomedical Research and the Department of Biology, Massachusetts Institute of Technology, Cambridge, MA 02142, USA
[6]Department of Biological Sciences, Florida International University, Miami, FL 33199, USA
[7]State Key Laboratory of Experimental Hematology, Institute of Hematology and Blood Diseases Hospital, Chinese Academy of Medical Sciences and Peking Union Medical College, Tianjin 300020, China
[8]Department of Biostatistics and Bioinformatics, Rollins School of Public Health, Emory University, Atlanta, GA 30322, USA
[9]Department of Pathology, University of Illinois at Chicago, Chicago, IL 60612, USA
[10]Co-first author
*Correspondence: jaenisch@wi.mit.edu (R.J.), peng.jin@emory.edu (P.J.), mxx51@miami.edu (M.X.)
http://dx.doi.org/10.1016/j.celrep.2015.10.037

SUMMARY

TET1/2/3 are methylcytosine dioxygenases that regulate cytosine hydroxymethylation. Tet1/2 are abundantly expressed in HSC/HPCs and are implicated in hematological malignancies. *Tet2* deletion in mice causes myeloid malignancies, while *Tet1-null* mice develop B cell lymphoma after an extended period of latency. Interestingly, *TET1/2* are often concomitantly downregulated in acute B-lymphocytic leukemia. Here, we investigated the overlapping and non-redundant functions of Tet1/2 using *Tet1/2* double-knockout (*DKO*) mice. *DKO* and *Tet2*$^{-/-}$ HSC/HPCs show overlapping and unique 5hmC and 5mC profiles. *DKO* mice exhibit strikingly decreased incidence and delayed onset of myeloid malignancies in comparison to *Tet2*$^{-/-}$ mice and in contrast develop lethal B cell malignancies. Transcriptome analysis of *DKO* tumors reveals expression changes in many genes dysregulated in human B cell malignancies, including *LMO2*, *BCL6*, and *MYC*. These results highlight the critical roles of TET1/2 individually and together in the pathogenesis of hematological malignancies.

INTRODUCTION

The ten-eleven translocation (TET) family of proteins is composed of three members, TET1, TET2, and TET3 (Iyer et al., 2009; Tahiliani et al., 2009). They share a conserved Cys-rich domain and double-stranded beta helix domain (Iyer et al., 2009). TETs exhibit their unique enzymatic function and facilitate DNA demethylation, oxidizing 5-methylcytosine (5mC) to 5-hydroxymethylcytosine (5hmC), 5-formylcytosine (5fC), and 5-carboxylcytosine (5caC) in a stepwise manner (He et al., 2011; Ito et al., 2011; Tahiliani et al., 2009). TETs can thus act as epigenetic regulators and modulate gene transcription and cellular functions (Pastor et al., 2013).

Mutations and/or deletions of the *TET2* gene have been reported to frequently occur in multiple myeloid malignancies, including approximately 30% of myelodysplastic syndromes (MDS), 20% of myeloproliferative neoplasms (MPN), 17% of de novo acute myeloid leukemias (AML), 30% of secondary AMLs, and 50%–60% of chronic myelomonocytic leukemias (CMMLs) (Delhommeau et al., 2009; Jankowska et al., 2009; Langemeijer et al., 2009). *TET2* mutations have also been found in approximately 2% of Hodgkin's lymphoma cases and 11.9% of T cell lymphoma patients (Quivoron et al., 2011). In addition, Musialik et al. recently showed that *TET2* expression is significantly lower in acute B-lymphocytic leukemia (B-ALL) patients when compared to control CD19^{+} samples. *TET1* was first identified as a fusion partner of the mixed lineage leukemia (*MLL*) gene in AML patients carrying t(10,11)(q22;q23) (Ono et al., 2002). Recently, *TET1* was shown to be transcriptionally downregulated in human B cell non-Hodgkin lymphomas (B-NHL), including diffuse large B cell lymphoma (DLBCL) and follicular lymphoma (FL) (Cimmino et al., 2015). Huang et al. reported that *TET1* is significantly upregulated and plays an oncogenic role in MLL-rearranged leukemia, rendering TET1 as a potential target for treating this form of hematopoietic malignancy (Huang et al., 2013). However, Cimmino et al. recently showed that deletion of *Tet1* promoted the development of B cell lymphoma in

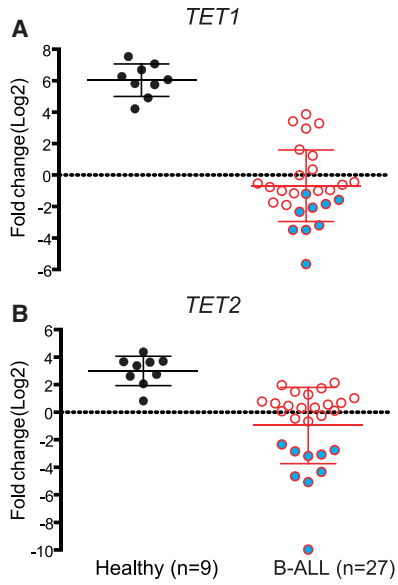

Figure 1. Analyses of *TET1* and *TET2* Gene Expression in Human Acute B-Lymphocytic Leukemia Patients

qRT-PCR analysis of *TET1* (A) and *TET2* (B) expression in peripheral blood (PB) mononuclear cells from B-ALL patients (n = 27) and PB $CD19^+$ cells from healthy controls (n = 9). Patients with concurrent *TET1* and *TET2* downregulation are marked with a blue dot (n = 9). The relative mRNA expression of each *TET* gene was determined using *GAPDH* as internal calibrator. The mRNA expression levels are reported as relative expression units to the respective *TET* expression in a B-ALL patient with the middle range *TET1* or *TET2* expression.

mice (Cimmino et al., 2015). These studies indicate that TET1 may play an oncogenic or tumor suppressive role in a cell-type-specific fashion.

Both Tet1 and Tet2 are abundantly expressed in hematopoietic stem/progenitor cells (HSC/HPCs) and differentiated lineages such as B cells and myeloid cells (Huang et al., 2013; Li et al., 2011; Moran-Crusio et al., 2011). Tet2 plays a prominent and essential role in HSC self-renewal, proliferation, and differentiation, and Tet2 loss leads to an increased HSC self-renewal and skewed differentiation favoring monocytic lineage (Ko et al., 2011; Li et al., 2011; Moran-Crusio et al., 2011; Quivoron et al., 2011). Furthermore, $Tet2^{-/-}$ mice develop myeloid malignancies including CMML, MPN-like myeloid leukemia, and MDS (Li et al., 2011; Moran-Crusio et al., 2011; Quivoron et al., 2011). Tet2, therefore, acts as a tumor suppressor in myelopoiesis.

Given the abundant expression of both Tet1 and Tet2 along the HSC differentiation hierarchy, Tet1 and Tet2 can have both non-redundant and overlapping functions in regulating HSC maintenance, hematopoietic homeostasis, and leukemogenesis. Interestingly, *TET1* and *TET2* are often concomitantly downregulated in B-ALL. Therefore, it is important to investigate the effects of combined loss of Tet1/2 on the hematopoietic phenotype and development of hematological malignancies in vivo. Here, we report that combined deficiency of Tet1/2 causes mainly B cell malignancies in *DKO* mice with a strikingly decreased frequency and delayed onset of myeloid malignancies compared to $Tet2^{-/-}$ mice. $Tet2^{-/-}$ and *DKO* HSC/HPCs displayed distinct DNA 5hmC/5mC signatures, which does not correlate with gene expression alteration. Transcriptome analysis of *DKO* tumors revealed altered expression in many genes dysregulated in human B cell malignancy, including *LMO2*, *BCL6*, and *MYC*. These findings provide a framework for further studies on molecular mechanisms that critically link TET1 and TET2 in the pathogenesis of hematological malignancies.

RESULTS

TET1 and *TET2* Are Often Concomitantly Downregulated in Human Acute B-Lymphocytic Leukemia Patients

TET2 is frequently mutated in both myeloid and lymphoid malignancies, whereas *TET1* mutations are rare. We first examined by quantitative real-time PCR the mRNA expression of *TET1* and *TET2* in peripheral blood (PB) mononuclear cells from a cohort of B-ALL patients, and compared it with that of PB $CD19^+$ B cells from healthy controls. Downregulation of *TET1* mRNA expression was observed in 21 of the 27 B-ALL patients as compared to healthy controls (Figure 1A), while downregulation of *TET2* was noted in nine of the 27 B-ALL patients (Figure 1B). Interestingly, all of the nine B-ALL patients with *TET2* downregulation had concomitant *TET1* downregulation (Figures 1A and 1B). These data suggest that combined *TET1* and *TET2* loss may play important roles in the pathogenesis of B cell malignancies and prompted us to examine the hematological phenotype displayed in *Tet1/2 DKO* mice.

Tet1/2 DKO Mice Develop Lethal B Cell Malignancies

Analysis of hematological parameters on young wild-type (WT), $Tet1^{-/-}$, $Tet2^{-/-}$, and *DKO* mice showed that up to 4 months of age *DKO* mice do not exhibit signs of CMML development that $Tet2^{-/-}$ mice display at this age (Figure S1) (Li et al., 2011). To determine whether *DKO* mice develop hematological malignancies later in life, we aged a cohort of WT, $Tet1^{-/-}$, $Tet2^{-/-}$, and *DKO* mice. Analysis of total blood counts and blood smears of 12- to 15-month-old $Tet2^{-/-}$ mice revealed features that are consistent with development of myeloid malignancies. Most of the aged $Tet2^{-/-}$ mice displayed significantly higher WBC counts (mainly caused by neutrophilia and monocytosis), compared to age-matched WT mice (Figures 2A and 2B). The blood cell counts of aged $Tet1^{-/-}$ mice were comparable to those of WT mice (Figure 2A). In contrast, 12 of the 19 aged *DKO* mice exhibited increased WBC counts, with 11 caused by marked lymphocytosis but normal monocyte and neutrophil counts (Figures 2A and 2B). Only one of these *DKO* mice (G3-21) displayed prominent neutrophilia and monocytosis but normal lymphocyte count. Two of the 19 *DKO* (10.6%) and three of the 14 $Tet2^{-/-}$ (21.4%) mice were anemic, evidenced by reduced RBC counts. PB smears from most of the *DKO* mice showed absolute lymphocytosis with predominantly intermediate to large-sized lymphocytes containing a small amount of cytoplasm and slightly irregular and dispersed nuclear chromatin (Figure 2B). Interestingly, 68.4% of the *DKO* mice either became moribund or died within 20 months of their life, whereas none of the WT, 7.6% of $Tet1^{-/-}$, and 90% of $Tet2^{-/-}$ mice died at the endpoint of our evaluation (Figure 2C; Table S1). Necropsy of the moribund/deceased *DKO* mice revealed pronounced

hepatosplenomegaly in all and enlarged lymph nodes in most of the mice (Figure 2D; Table S1). Flow cytometric analyses on PB, spleen, and BM cell preparations from the moribund/deceased *DKO* mice revealed predominant proportions of $B220^{+}IgM^{+/low}CD43^{+}CD19^{+}$ B-lymphocytes with high forward scatter (FSC) in nine of the ten *DKO* mice, demonstrating a neoplastic monomorphic expansion of B cell origin (Figures 2E, S2A, and S2B; Table S1). Furthermore, the neoplastic B-lymphocytes expressed CD71 in all and CD5 in two-thirds of the *DKO* mice (Figure S2B; Table S1). In each of the *DKO* mice with predominant neoplastic B cells, the proportion of myeloid and T cells in the PB, BM, and spleen were either decreased or comparable to WT mice (Figure S2C), which is likely related to the predominance of B cell populations rather than a primary defect. Note that in one moribund *DKO* animal (G3-21) with monocytosis/neutrophilia, its BM and spleen cells showed predominant proportions of $CD11b^{+}F4/80^{+}Gr\text{-}1^{low}$ monocytic cell populations (Table S1), indicating CMML.

Examination of H&E-stained BM, spleen, liver, and lymph node sections and May-Giemsa-stained cytospin preparations of BM and spleen cells from the moribund/deceased *DKO* mice revealed extensive infiltration with intermediate to large-sized immature-appearing lymphocytes with large nuclei and small amount of cytoplasm, slightly irregular nuclei and dispersed nuclear chromatin (Figures 2F and S2D). BM showed diffuse neoplastic lymphoid infiltration with decreased normal trilineage hematopoiesis (Figure 2F). The normal architecture of spleen and lymph nodes was effaced and replaced by diffuse atypical lymphoid infiltrates (Figure 2F). Both red and white pulp of the spleen were involved. The liver displayed nodular and sinusoidal lymphoid infiltration, which was also confirmed by immunostaining with anti-B220 and anti-CD43 antibodies (Figures 2F and 2G). Furthermore, to determine whether these monotypic expansions/infiltrations were clonal, PCR analysis of immunoglobulin H (IgH) D-J rearrangements was performed. Clonal gene rearrangements were detected for IgD-J junctions in five of six mice tested. Splenic B cells from three *DKO* mice showed monoclonal Ig rearrangements. Two mice demonstrated biclonal Ig rearrangements. These Ig gene rearrangement assays revealed that the splenic $B220^{+}$ cells from each of these *DKO* mice with monomorphic B cell expansions/infiltrations were clonal, while $B220^{+}$ cells from the *DKO* case with CMML or WT displayed oligoclonal patterns (Figure 2H). Collectively, the majority of these aged *DKO* mice developed B cell malignancy, with features most closely resembling human B-ALL (Table S1).

B Cell Malignancy in *DKO* Mice Is Transplantable to Secondary Recipients

To evaluate the malignant nature of the abnormally infiltrated B-lymphocytes in *DKO* mice, spleen cells from a moribund *DKO* (G2-53) and a WT mice were transplanted into sublethally irradiated WT recipients (Figure S3A). None of the recipients receiving WT spleen cells developed pathology or gross evidence of disease within 4 months of transplantation (Figures 3A–3D). In contrast, all of the mice receiving *DKO* spleen cells developed diseases with similar characteristics as those observed in the primary mouse including elevated WBC counts, lymphocytosis, splenomegaly, enlarged lymph nodes, and death (Figures 3A, 3B, S3B, and S3C). Flow cytometric analysis and histological and cytospin examination of PB, spleen, BM, liver, lymph node, lung, and kidney cells of the recipients revealed predominant infiltration of a uniform B cell population (high FSC, $B220^{+}CD19^{+}IgM^{+/low}CD43^{+}CD5^{+}CD71^{+}$) similar to that observed in the primary *DKO* mouse (Figures 3C, 3D, S3D, and S3E; data not shown). These data demonstrate that the *Tet1/2*-deletion-induced B cell malignancy is transplantable, suggesting a malignant and neoplastic nature of the infiltrated B cells in *DKO* mice.

In addition, long-term observation of a cohort of $Tet1^{+/-}$; $Tet2^{-/-}$ mice (n = 15) showed that $Tet1^{+/-}$;$Tet2^{-/-}$ mice have an improved survival rate compared to $Tet2^{-/-}$ mice, but a comparable survival rate compared to *DKO* mice (Figure S2E; Table S2). Interestingly, analysis of nine moribund/deceased $Tet1^{+/-}$; $Tet2^{-/-}$ mice demonstrate that seven of nine developed B cell malignancy (B-ALL) and two of nine developed myeloid malignancies (Figure S2F; Table S2). Our long-term observation of 196 $Tet2^{-/-}$ mice demonstrate that ~93% of $Tet2^{-/-}$ mice developed myeloid malignancies and only ~4% developed B cell malignancies (Figure S2F; our unpublished data). These data indicate that Tet1 loss modulates *Tet2*-deletion-mediated disease phenotype in mice, not only decreasing the incidence and delaying the onset of myeloid malignancies, but also promoting the pathogenesis of B cell malignancies.

Deletion of *Tet1/2* Increases CLP/BLP Compartment and Affects B Cell Development in Mice

To explore the cellular mechanisms by which deletion of *Tet1/2* causes high frequency of B cell malignancies but low frequency of myeloid malignancies, we analyzed HSC, myeloid, and lymphoid progenitors and various maturation stages of B cell populations in the BM of 5- to 7-week-old *DKO* mice prior to their development of hematological malignancies. The proportion of LSK cells and each of the myeloid progenitors (CMP, GMP, and MEP) was comparable to WT, $Tet1^{-/-}$, and *DKO* mice, whereas LSK and GMP cell populations were significantly increased in $Tet2^{-/-}$ mice (Figures 4A and 4B; data not shown). Similar results were obtained with conditional *MxCre*-mediated *Tet1* and/or *Tet2* deletion in adult mice (Figures S4 and S5). $Tet2^{f/f}$;*MxCre* mice had increased LSK and GMP cell populations compared to that of $Tet1^{f/f}$;$Tet2^{f/f}$;*MxCre*, $Tet1^{f/f}$;*MxCre* and $Tet1^{f/f}$;$Tet2^{f/f}$ mice 5–6 weeks after *pI:pC* injection (Figures S5A–S5D).

We also assessed the replating potential of purified LSK cells from 5- to 7-week-old WT, $Tet1^{-/-}$, $Tet2^{-/-}$, and *DKO* mice by in vitro myeloid colony formation assays. A significant increase in colony formation was observed for $Tet2^{-/-}$ LSK cell cultures in each round of replating, while $Tet1^{-/-}$ and *DKO* LSK cell cultures exhibited a moderate increase in the number of colonies at P2, but not P3 and P4 (Figure 4C). Furthermore, re-introduction of WT Tet1, but not catalytic domain inactive mutant Tet1, into *DKO* LSK cells significantly increased their replating potential at P2-P4 (Figures S5E and S5F). These data suggest that Tet1 loss abrogated the *Tet2*-deletion-caused LSK pool increment in vivo and their hyper-replating potential in vitro. In addition, the catalytic activity of Tet1 is likely required for Tet2 loss-induced hyper-replating potential in HSC/HPCs.

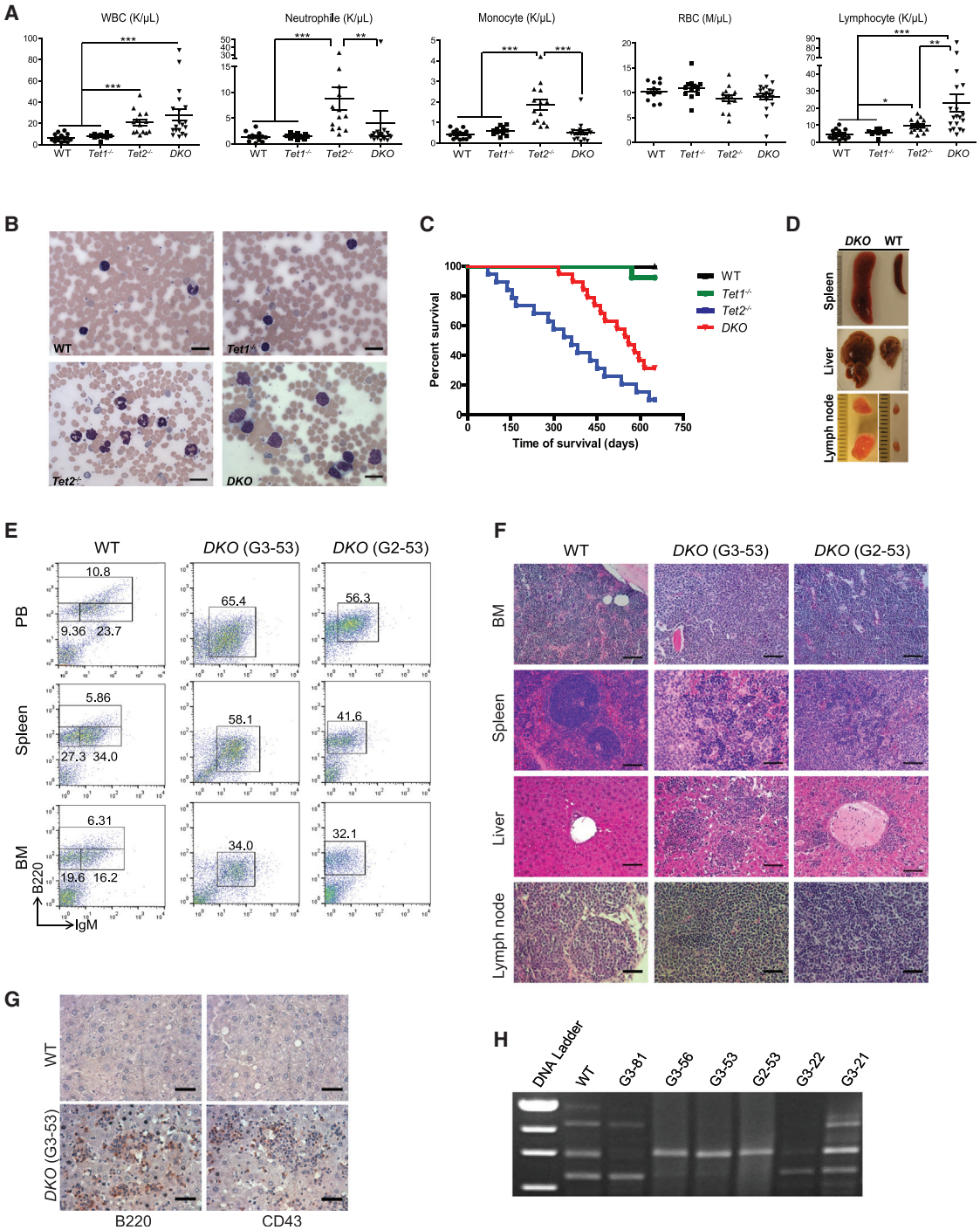

Figure 2. Most of the *DKO* Mice Developed Lethal B-Lymphoid Malignancies

(A) Most of the aged *DKO* mice exhibited elevated WBC and lymphocyte counts. WBC, neutrophil, monocyte, lymphocyte, and RBC counts were performed with 12- to 15-month-old *DKO* mice (n = 19) and age-matched WT (n = 13), *Tet1*$^{-/-}$ (n = 12), and *Tet2*$^{-/-}$ (n = 14) mice. *p < 0.05, **p < 0.01, ***p < 0.001.

(B) May-Giemsa-stained PB smears prepared from a representative moribund *DKO* mouse and age-matched WT, *Tet1*$^{-/-}$ and *Tet2*$^{-/-}$ mice. Bar, 20 μm.

(C) Kaplan-Meier survival curve of WT (n = 25), *Tet1*$^{-/-}$ (n = 13), *Tet2*$^{-/-}$ (n = 20), and *DKO* (n = 19) mice up to 650 days.

(D) The gross morphologies of spleen, liver, and lymph nodes from a representative moribund *DKO* and an age-matched WT mouse.

(E) Flow cytometric analysis of B cell lineage (B220/IgM) in PB, BM, and spleen of representative moribund *DKO* (#G3-53 and #G2-53) and age-matched WT mice. The numbers indicate the percentages of cells in each cell population.

(legend continued on next page)

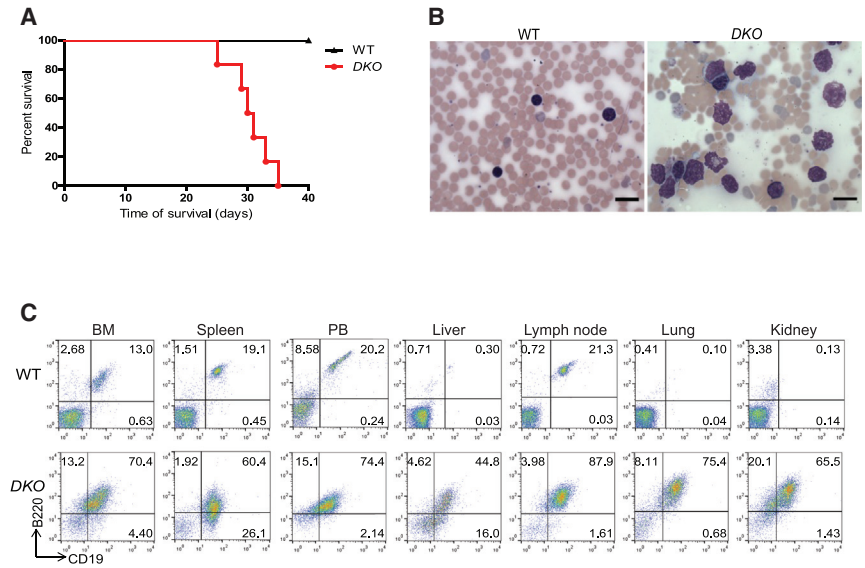

Figure 3. The B Cell Malignancy in *DKO* Mice Is Transplantable to Secondary Recipients

(A) Kaplan-Meier survival curve of sub-lethally irradiated recipients (six mice/donor) transplanted with spleen cells (1×10^6) from a WT mouse or a *DKO* mouse with B cell malignancy (G2-53).

(B–D) May-Giemsa-stained PB smear (B), flow cytometric analyses on B cell lineage (C), and H&E-stained histological sections (D, bar: 100 μm) of femurs, spleen, liver, lymph node, kidney, and lung from a representative recipient mouse receiving spleen cells from a WT mouse or a *DKO* mouse with B cell malignancy. Neoplastic lymphocytic infiltrates were identified in each of the organs. Infiltrating patterns and cell morphology were similar to those observed in the donor *DKO* mice. These data demonstrate that the recipients receiving spleen cells from the *DKO* mouse with B cell malignancy developed a disease similar to their donor mouse.

Interestingly, a significantly increased frequency of common lymphoid progenitors (CLPs) and B-lymphocyte progenitors (BLP) is observed in *DKO* mice (5–7 weeks old), whereas comparable CLP and BLP frequencies are seen in *Tet1*$^{-/-}$, *Tet2*$^{-/-}$, and WT mice (Figures 4D–4F). In addition, when BM cells of young WT, *Tet1*$^{-/-}$, *Tet2*$^{-/-}$, and *DKO* mice are examined for their Pro-, Pre-, Immature-, and Mature-B cell populations, *DKO* mice show significantly higher frequencies of Pro-, Pre-, and Immature-B cells, but not mature-B cells, whereas, *Tet1*$^{-/-}$ mice show higher frequencies of Immature-B cells in comparison to WT control mice (Figures 4G and 4H). Frequencies for each B cell population is comparable or slightly decreased in *Tet2*$^{-/-}$ mice in comparison to WT mice (Figures 4G and 4H), which might be related to an increased Gr1/Mac1 cell population in their BM. Consistently, B cell colony formation assay shows significantly increased B cell colonies in the BM of *DKO* mice compared to *Tet1*$^{-/-}$, *Tet2*$^{-/-}$, and WT mice (Figure 4I). A moderate increase in B cell colony formation is also seen in *Tet1*$^{-/-}$ and *Tet2*$^{-/-}$ mice compared to WT controls (Figure 4I). These results indicate that deletion of both *Tet1/2* results in increased CLP, BLP, and Pro-/Pre-/Immature-B cell populations in vivo (Figure 4J), which might predispose and/or facilitate the development of B cell malignancies.

Tet1/2-Deficient HSCs Exhibit an Increased Short-Term, but Not Long-Term, Hematopoietic Repopulating Capacity

To determine whether deletion of *Tet1/2* affects HSC activity in a cell intrinsic manner in vivo, we performed a competitive BM reconstitution assay by transplanting total CD45.2$^+$ nucleated BM cells (1×10^6) from 6- to 7-week-old *Tet1*$^{f/f}$;*Tet2*$^{f/f}$, *Tet2*$^{f/f}$;*MxCre*, or *Tet1*$^{f/f}$;*Tet2*$^{f/f}$;*MxCre* mice along with an equal number of WT CD45.1$^+$ BM cells, into lethally irradiated F1 recipient mice (Figure 5A). Four weeks after transplantation, the recipients were assessed for CD45.2/CD45.1 chimeras in their PB by FACS analysis and then were induced for *Tet1* and/or *Tet2* deletion by *pI:pC* injections. The contribution of CD45.1$^+$ versus CD45.2$^+$ cells in the PB was monitored every 4 weeks for 28 weeks after *pI:pC* injections. CD45.2$^+$ *Tet1*$^{f/f}$;*Tet2*$^{f/f}$ cell chimeras remained around 50%, whereas there was a steady increase in the CD45.2$^+$ *Tet2*$^{f/f}$;*MxCre* cell chimeras that reached over 70% at 28 weeks. Interestingly, *Tet1*$^{f/f}$;*Tet2*$^{f/f}$;*MxCre* cell chimeras increased to ~60% during the first 16 weeks and then slightly declined with no significant differences compared to *Tet1*$^{f/f}$;*Tet2*$^{f/f}$ CD45.2$^+$ cell chimeras at 24 and 28 weeks. The *Tet1*$^{f/f}$;*Tet2*$^{f/f}$;*MxCre* cell chimeras were significantly smaller than that of *Tet2*$^{f/f}$;*MxCre* cells after 20 weeks (Figures 5B and 5C). Furthermore, *Tet2*$^{f/f}$;*MxCre*, but not *Tet1*$^{f/f}$;*Tet2*$^{f/f}$;*MxCre* BM cells contributed to a greater proportion of Gr1/Mac1

(F) H&E-stained histological sections of femurs, spleen, liver, and lymph node (bar, 100 μm) from representative moribund *DKO* (#G3-53 and #G2-53) and age-matched WT mice.

(G) Liver sections from a representative moribund *DKO* (#G3-53) and WT mouse were immunostained using anti-B220 or CD43 antibodies.

(H) The D-J rearrangement of the IgH gene in splenic cells from *DKO* (n = 6) and WT mice.

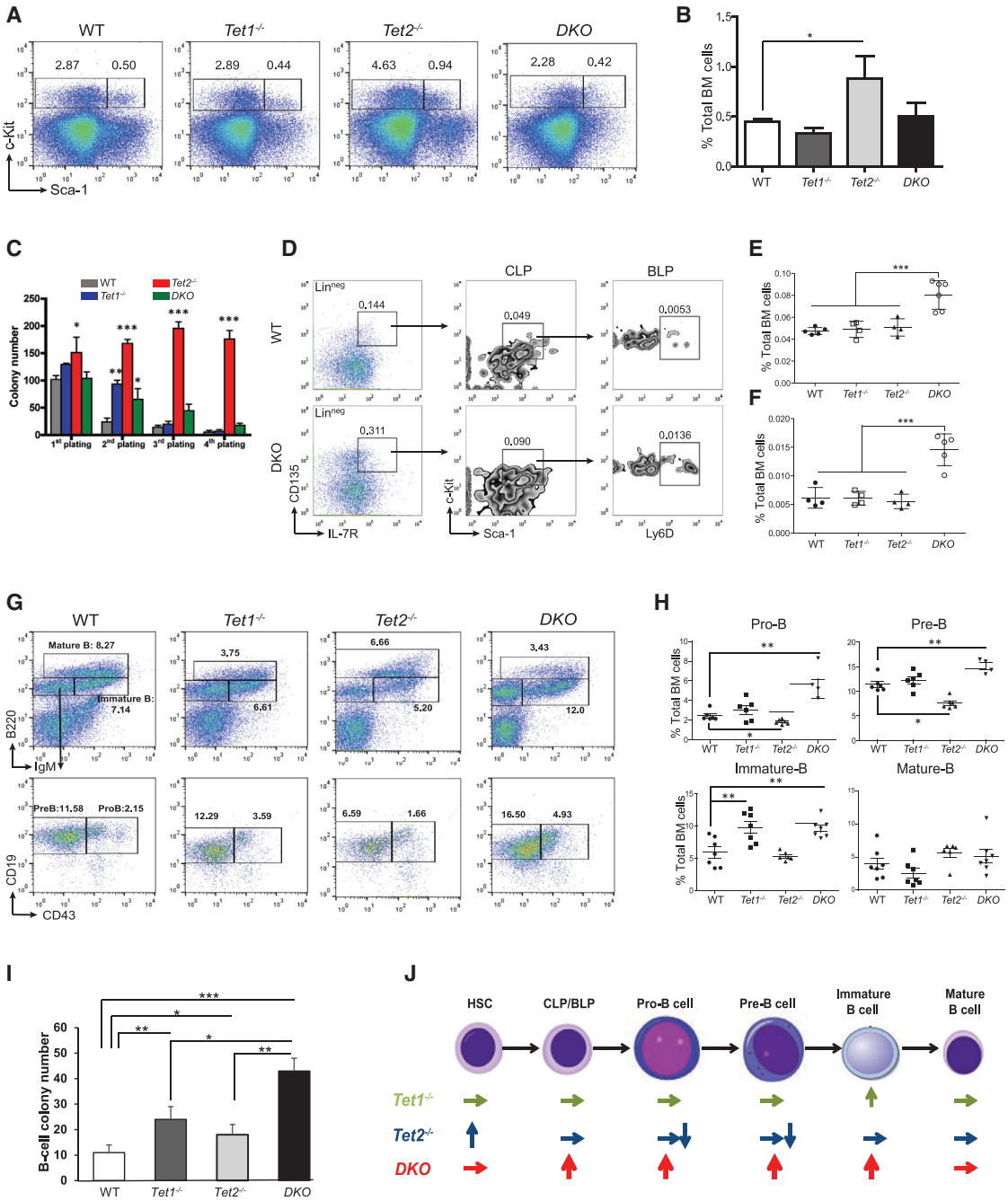

Figure 4. Frequencies of HSC, Myeloid, and Lymphoid Progenitor Compartments, as well as Various B Cell Sub-populations in *DKO* Mice

(A) Flow cytometric analysis of Sca-1$^+$c-Kit$^+$ and Sca-1$^-$c-Kit$^+$ cell populations in the total BM cells of representative WT, *Tet1*$^{-/-}$, *Tet2*$^{-/-}$, and *DKO* mice (7 weeks old).

(B) Quantitation of the percentage of Sca-1$^+$c-Kit$^+$ cells in the BM of each mouse genotype (mean ± SD, four to five mice/genotype).

(C) Colony-formation assay of LSK cells sorted from each genotype of BM cells in methylcellulose medium (500 cells/plate). Colonies were passaged every 7 days for three sequential platings (P1-4). Data are representative of three experiments.

(D) Flow cytometric analysis of common lymphoid progenitors (CLP, Lin$^-$IL-7R$^+$CD135$^+$c-kit^{low}Sca-1^{low}) and B-lymphocyte progenitors (BLP, Lin$^-$IL-7R$^+$CD135$^+$Ly6D$^+$c-kit^{low}Sca-1^{low}) in the BM of representative WT and *DKO* mice.

(E and F) Quantitation of the percentage of CLP (E) and BLP (F) in the total BM cells of each mouse genotype (mean ± SD, five to six mice/genotype).

(G) Flow cytometric analysis of Pro-B (B220$^+$IgM$^-$CD19$^+$CD43$^+$), Pre-B (B220$^+$IgM$^-$CD19$^+$CD43$^-$), Immature-B (B220$^+$IgM$^+$), and Mature-B (B220$^+$IgM^{low}) cell populations in the BM cells of representative WT, *Tet1*$^{-/-}$, *Tet2*$^{-/-}$, and *DKO* mice (7 weeks old).

(H) Quantitation of the percentage of Pro-B, Pre-B, Immature-B, and Mature-B cells in the total BM cells of each genotype of mice (mean ± SD, four to seven mice/genotype).

(legend continued on next page)

granulocytic/monocytic cells and a smaller proportion of B220$^+$ B cells in the recipient BM compared to controls (Figure 5D).

Consistent with PB, at 24 weeks after *pI:pC* injections, CD45.2 chimeras in the BM was also significantly higher in *Tet2$^{f/f}$;MxCre* BM transplants than *Tet1$^{f/f}$;Tet2$^{f/f}$;MxCre* or *Tet1$^{f/f}$;Tet2$^{f/f}$* BM transplants (Figures 5E and 5F). Furthermore, within the CD45.2$^+$ BM cell populations, the frequencies of LSK and GMP, but not CLP were increased in *Tet2$^{f/f}$;MxCre* BM transplants, whereas the frequency of CLP, but not LSK and GMP, was increased in *Tet1$^{f/f}$;Tet2$^{f/f}$;MxCre* BM transplants as compared to the control *Tet1$^{f/f}$;Tet2$^{f/f}$* BM transplants (Figures 5G–5I). These data suggest that *Tet1/2* deletion in HSC/HPCs moderately increases their short-term, but not long-term repopulating capacity while promoting the CLP expansion. The data also confirm previous observations that *Tet2*-deficient HSCs exhibit an enhanced HSC activity and skewed differentiation toward granulocytic/monocytic lineage.

In addition, three of the five mice receiving *Tet2$^{f/f}$;MxCre* BM cells had moderate monocytosis and splenomegaly 24 weeks after *pI:pC* injections (Figure 5J; data not shown), reminiscent of the CMML phenotype displayed in *Tet2$^{-/-}$* mice. Furthermore, two of the five mice receiving *Tet1$^{f/f}$;Tet2$^{f/f}$;MxCre* BM cells had mild lymphocytosis and splenomegaly (Figure 5I; data not shown), reminiscent of the B cell malignancy phenotype displayed in *DKO* mice. None of the mice receiving *Tet1$^{f/f}$;Tet2$^{f/f}$* BM cells developed any signs of hematological malignancies. These data suggest that the *Tet1/2*-deletion-induced phenotype is likely cell autonomous.

Tet2$^{-/-}$ and *DKO* LK Cells Display Distinct DNA Methylation/Hydroxymethylation Signatures

Given the role of Tet proteins in 5mC oxidation, we employed a previously established chemical labeling and affinity purification method coupled with high-throughput sequencing (hMe-Seal) to profile the genome-wide distribution of 5hmC. We also used methylated DNA immunoprecipitation (MeDIP) coupled with high-throughput sequencing (MeDIP-seq) to profile 5mC using BM LK cells purified from young WT, *Tet2$^{-/-}$*, and *DKO* mice (5–8 weeks old). The loss of Tet2 or Tet1/2 leads to genome-wide alterations of both 5mC and 5hmC (Figure 6A). We observed significant overlap in differential hydroxymethylated regions (DhMRs) or differential methylated regions (DMRs) between the two genotypes of LK cells (Figures 6B and S6A). Intriguingly, the overlap between DhMRs and DMRs within each genotype of LK cells was minimal, indicating that DhMRs and DMRs might represent distinct loci with altered epigenetic modifications under these conditions (Figures 6C and S6B).

To further explore molecular mechanisms underlying phenotypes associated with these two mutant lines of mice, we applied RNA sequencing (RNA-seq) to the LK cells from young *Tet2$^{-/-}$* and *DKO* mice that we used for epigenomic analyses. We primarily focused on 654 genes that are known to be involved in regulating hematopoietic cell development and/or to promote leukemogenesis, based on previously published studies (Abdel-Wahab et al., 2013; Chambers et al., 2007; Shlush et al., 2014). By overlapping with the DhMRs or DMRs identified above, we observed a significant number of these genes with altered 5hmC or 5mC modifications (Figures 6D and S6C–S6E). However, we did not observe significant expression changes in these genes in either *Tet2$^{-/-}$* or *DKO* LK cells, and there was no clear correlation between gene expression changes and the 5hmC/5mC alteration (Figures 6E and 6F). This is consistent with previous findings that no direct correlation is observed between gene expression alteration and 5hmC changes in mouse ES cells (Ficz et al., 2011; Pastor et al., 2011; Williams et al., 2011). These observations suggest the roles of distinct cytosine modifications (particularly 5hmC) could play in marking specific genes, which may enable cells to respond to additional stimuli to subsequently altering gene expression.

Altered Expression of Genes Implicated in Human B Cell Malignancies in the B-ALL *DKO* B220$^+$ Cells

Next, we performed RNA-seq to identify the dysregulated genes in preleukemic and B-ALL *DKO* B220$^+$ cells. B220$^+$ cells were isolated from the spleen cells of B-ALL *DKO* mice, age-matched WT, and pre-leukemic *DKO* mice. RNA-seq analysis of preleukemic *DKO* B220$^+$ cells identified a pool of dysregulated genes, compared to WT B220$^+$ cells, which are implicated in B cell development such as *Sox4*, *Ets2*, and *Irf4* (Mallampati et al., 2014; Simonetti et al., 2013; Yoshimatsu et al., 2011), and consistent with the observation that impaired B cell development occurs in these *DKO* mice (Figure 7A). Moreover, analysis of the RNA-seq data identified a panel of differentially expressed genes in B-ALL *DKO* B220$^+$ cells compared to WT or pre-leukemic *DKO* B220$^+$ cells. When compared to pre-leukemic *DKO* B220$^+$ cells, 294 genes were upregulated and 205 genes were downregulated in B-ALL *DKO* B220$^+$ cells (false discovery rate [FDR] <0.05). The significantly altered genes in B-ALL *DKO* B220$^+$ cells included many dysregulated genes in human B cell malignancy such as *Lmo2*, *Bcl6*, *Myc*, *Pten*, and *Blk* (Natkunam et al., 2007; Ott et al., 2013; Pfeifer et al., 2013), further validating B cell malignancy occurring in these B-ALL *DKO* mice (Figure 7B).

We then integrated the previously published TET1 and TET2 chromatin immunoprecipitation sequencing (ChIP-seq) data with our RNA-seq data to search for known TET1 target genes (Williams et al., 2011) and TET2 target genes (Deplus et al., 2013) within the significantly dysregulated genes in B-ALL *DKO* B220$^+$ cells. Interestingly, nearly 40% of these dysregulated genes were direct targets of TET1 (such as *Jun*, *Myc*, and *Lmo2*), and ~10% were direct targets of TET2 (such as *Pbx3*, *Rras2*, and *Flt3*) (Figure 7C). These data suggest that Tet1 and/or Tet2 are capable of regulating the expression of these genes in the transformed B-ALL *DKO* B220$^+$ cells, and Tet1 seems more capable of controlling its target gene expression

(I) Pre-B colony-formation assays of BM cells from each mouse genotype. Colonies were scored after 12–14 days of culture. Data are representative of three experiments.

(J) Schematic overview of the effects of *Tet1* and/or *Tet2* deletion on B cell development/maturation.

*p < 0.05, **p < 0.01, ***p < 0.001.

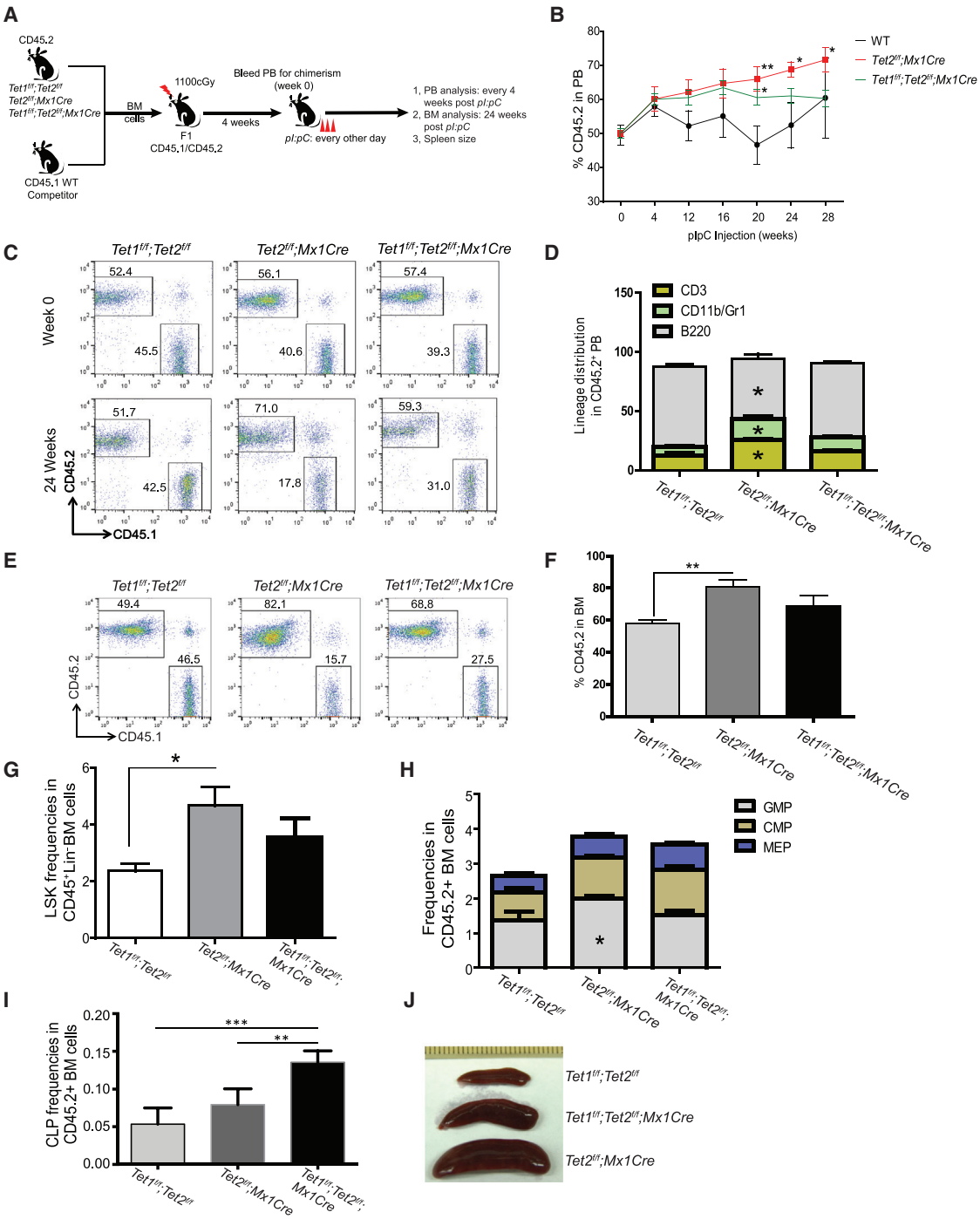

Figure 5. Hematopoietic Repopulating Capacity of *DKO* HSCs

(A) Schematic depiction of the competitive transplantation scheme. CD45.2$^+$ BM cells from *Tet1$^{f/f}$;Tet2$^{f/f}$*, *Tet2$^{f/f}$;MxCre*, and *Tet1$^{f/f}$;Tet2$^{f/f}$;MxCre* mice were mixed with CD45.1$^+$ competitor cells at a ratio of 1:1 (1 × 10^6 cells each) and transplanted into lethally irradiated F1 recipients. Recipients were injected with *pI:pC* 4 weeks after transplantation to induce *MxCre*-mediated *Tet1/2* deletion in the CD45.2$^+$ donor cells.

(B) The kinetics of the CD45.2$^+$ cell chimerism in the PB of mice receiving each genotype of BM cells. Data are shown as mean ± SD from four to seven animals/genotype.

(C) Flow cytometric analysis of PB cells from representative recipients of each group at 0 or 24 weeks after *pI:pC* injection.

(D) The lineage distribution within the PB CD45.2$^+$ cells of each group of recipients 24 weeks after *pI:pC* injection (mean ± SD from four to seven animals/genotype).

(E and F) The CD45.2$^+$ cell chimerism in the BM of mice receiving each genotype of BM cells 24 weeks after *pI:pC* injection (mean ± SD, three to five animals/genotype).

(legend continued on next page)

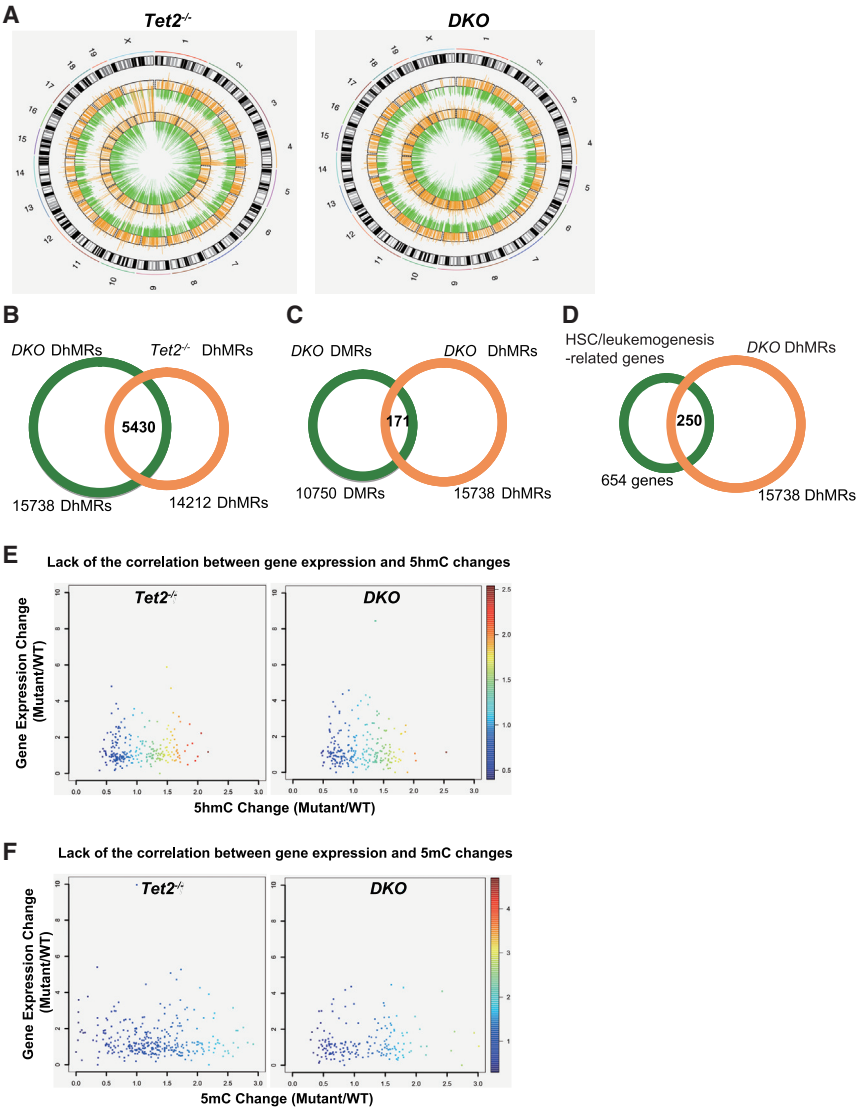

Figure 6. Distinct DhMRs/DMRs and Their Lack of Correlation with Gene Expression in *Tet2*$^{-/-}$ and *DKO* LK Cells

LK cells were sorted from the BM of WT, *Tet2*$^{-/-}$, and *DKO* mice (5–8 weeks old) and were analyzed for their 5mC and 5hmC profiling.

(A) Dynamic change of normalized 5hmC/5mC read counts ratio between Mutant (*Tet2*$^{-/-}$ and *DKO*) and WT cells in genome-wide DhMRs/DMRs. Chromosome circular map shows genome-wide dynamic change of normalized 5hmC/5mC read counts ratio between Mutant and WT cells in genome-wide DhMRs/DMRs. The outer track represents the normalized 5hmC read counts ratio between Mutant and WT cells in DhMRs. The inner track represents the normalized 5mC read counts ratio between Mutant and WT cells in DMRs. The orange color bar represents the normalized 5hmC/5mC read counts ratio in WT-specific DhMRs/DMRs. The green color bar represents the normalized 5hmC/5mC read counts ratio in Mutant-specific DhMRs/DMRs.

(B) Significant overlap between DhMRs of *Tet2*$^{-/-}$ and *DKO* LK cells. Venn diagram shows a significant overlap between the DhMRs identified in *DKO* versus WT cells and the DhMRs identified in *Tet2*$^{-/-}$ versus WT cells.

(C) Lack of overlap between DhMRs and DMRs for *DKO* LK cells. Venn diagram shows a lack of overlap between DhMRs and DMRs identified in *DKO* versus WT cells.

(D) Venn diagram shows the overlap between the HSC/leukemogenesis related gene bodies and DhMRs identified in *DKO* versus WT. A significant 250 out of 654 HSC/leukemogenesis related genes are overlapped with the DhMRs.

(E) The ratio of FPKM value of gene expression between Mutant (*Tet2*$^{-/-}$, *DKO*) and WT is plotted against the ratio of normalized 5hmC read counts between Mutant (*Tet2*$^{-/-}$, *DKO*) and WT. The lack of linear trend and significant deviation from the diagonal line suggest a lack of correlation between gene expression and 5hmC changes between Mutant (*Tet2*$^{-/-}$, *DKO*) and WT.

(F) The ratio of FPKM value of gene expression between Mutant (*Tet2*$^{-/-}$, *DKO*) and WT is plotted against the ratio of normalized 5mC read counts between Mutant (*Tet2*$^{-/-}$, *DKO*) and WT. The lack of linear trend and significant deviation from the diagonal line suggest a lack of correlation between gene expression and 5hmC changes between Mutant (*Tet2*$^{-/-}$, *DKO*) and WT.

compared to Tet2. These data also suggest that altered genes in B-ALL *DKO* B220^{+} cells are largely a direct result of combined Tet1/2 loss.

DISCUSSION

TET1/2/3 promote DNA demethylation by catalyzing conversion of 5mC primarily to 5hmC as well as 5-fC and 5-caC (He et al., 2011; Ito et al., 2011; Tahiliani et al., 2009). Previous work has shown that loss-of-function mutations of *TET2* frequently occur in myeloid malignancies (Delhommeau et al., 2009; Jankowska et al., 2009; Langemeijer et al., 2009), in which TET2 functions as a critical tumor suppressor (Li et al., 2011; Moran-Crusio et al., 2011; Quivoron et al., 2011). Somatic *TET2* mutations also occur in T cell lymphoma (such as angioimmunoblastic T lymphomas, 33%) and B-NHL (such as DLBCL, 12%; and mantle cell lymphoma, 4%). Besides loss-of-function mutations and deletions of *TET2*, TET2 inactivation or haploinsufficiency

(G–I) Flow cytometric analysis of LSK (G), GMP/MEP/CMP (H), and CLP (I) frequencies within the BM CD45.2^{+} cells of each group of recipients 24 weeks after *pI:pC* injection representative.

(J) Spleen size of representative mice receiving *Tet1*$^{f/f}$;*Tet2*$^{f/f}$, *Tet2*$^{f/f}$;*MxCre*, or *Tet1*$^{f/f}$;*Tet2*$^{f/f}$;*MxCre* BM cells 24 weeks after *pI:pC* injection.

*p < 0.05, **p < 0.01, ***p < 0.001.

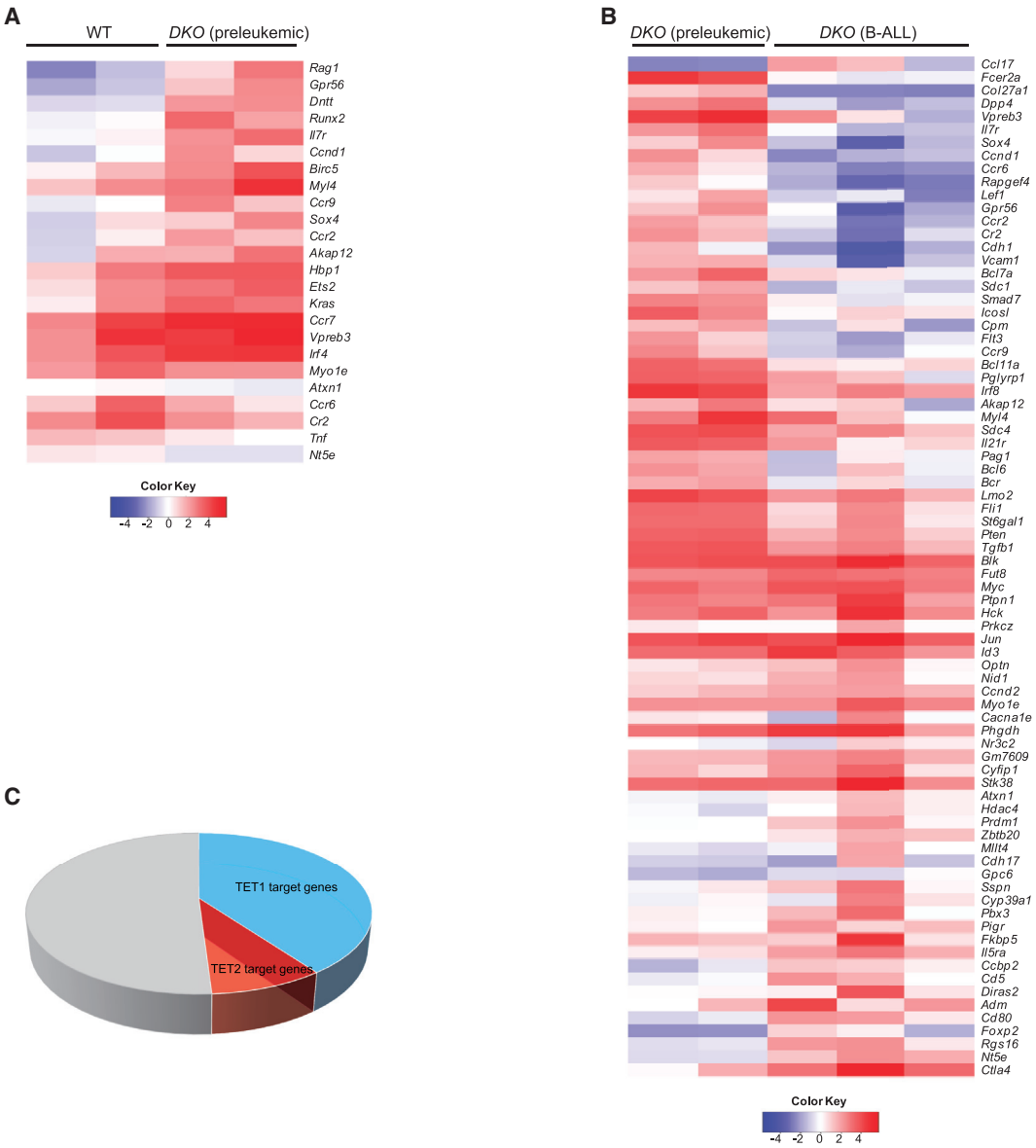

Figure 7. B-ALL *DKO* B220$^+$ Cells Had Altered Expression of Genes Implicated in Human B Cell Malignancies

(A) Heatmap of differentially expressed genes implicated in B cell development in preleukemic *DKO* B220$^+$ cells as compared to WT B220$^+$ cells (FDR <0.05, fold change >2, Log transformed data are presented).

(B) Heatmap of differentially expressed genes in B-ALL *DKO* B220$^+$ cells that are dysregulated in human B cell malignancies as compared to preleukemic *DKO* B220$^+$ cells (FDR <0.05, fold change > 2, Log transformed data are presented).

(C) Pie chart depicting the overlap of TET1-bound genes and TET2-bound genes within differentially expressed genes in B-ALL *DKO* B220$^+$ cells as compared to preleukemic *DKO* B220$^+$ cells. See Table S4 for a full list of differentially expressed genes and Table S5 for overlapping genes from RNA-seq and TET1/TET2 ChIP-seq data.

could result by other means such as gene downregulation. Indeed, TET2 mRNA expression level is significantly decreased in B-ALL compared to normal controls (Musialik et al., 2014). Our data show that *TET1* and *TET2* are often concomitantly downregulated in B-ALL patients. Recently, *TET1* was shown to be transcriptionally downregulated in B-NHL (DLBCL and FL) (Cimmino et al., 2015). Given the frequency of *TET2* mutations in these patients, *TET1* and *TET2* are likely simultaneously inactivated in some cases of B-NHL. Although the definitive function of TET1 in leukemogenesis remains to be determined, a recent study has implicated loss of Tet1 in onset of B cell lymphoma late in life (Cimmino et al., 2015). Nonetheless, Tet1 has also been implicated in an essential oncogenic role in *MLL*-rearranged leukemia (Huang et al., 2013). The seemingly opposite function of TET1 and TET2 in leukemogenesis and their combined inactivation in B cell malignancy pose a challenge to

the investigation of their overlapping and non-redundant roles in hematopoietic regulation and pathogenesis of hematological malignancies.

The generation of both germline and conditional *Tet1/2 DKO* mice has allowed us to gain valuable information toward addressing this important question and to determining the in vivo consequences of both TET1/2 loss in hematopoiesis and hematological malignancies. Our findings can be summarized as follows: (1) unlike *Tet2* deletion, deficiency of Tet1/2 does not cause an increased HSC pool in vivo and Tet1/2-deficient HSCs do not possess an increased long-term repopulating capability and skewed monocytic differentiation; (2) Tet1 loss dramatically decreases the incidence, and markedly delays the onset of *Tet2*-deletion-related myeloid malignancies; (3) deletion of both *Tet1/2* but not either in mice leads to increased CLP/BLP/Pro-B/Pre-B/Immature-B cell populations and results in the development of predominantly B-ALL; (4) $Tet2^{-/-}$ and *DKO* LK cells display distinct DNA methylation and hydroxymethylation signatures; however, no correlation between gene expression and DhMRs or DMRs is observed in both $Tet2^{-/-}$ and *DKO* HSC/HPCs; (5) transcriptome analyses of B-ALL *DKO* $B220^{+}$ cells identify alteration of genes that are dysregulated in human B cell malignancies such as *Lmo2*, *Bcl6*, *Myc*, *Pten*, and *Blk*.

Although TET2 is frequently mutated in T cell malignancies like angioimmunoblastic T lymphomas and peripheral T cell lymphoma (Sakata-Yanagimoto et al., 2014), and a fraction of $Tet2^{-/-}$ mice develop T cell malignancies (our unpublished data), none of the *DKO* mice we analyzed developed T cell malignancy, suggesting a low incidence of T cell malignancy in these mice. Future studies are required to determine the frequency of T cell malignancy in *DKO* mice.

Recent genome-wide profiling of 5mC distribution in murine HSC/HPCs highlights the significance of dynamic changes in DNA methylation (Bock et al., 2012; Sun et al., 2014), while little is known about 5hmC distribution in HSC/HPCs. Understanding the biological significance of 5mC and 5hmC dynamics and their relevance to TET1 and TET2 enzymes in HSC/HPCs is important. In this study, we demonstrate that the loss of Tet2 or Tet1/2 leads to genome-wide alterations of both 5mC and 5hmC. The significant amount of overlap of DhMRs or DMRs in LK cells between $Tet2^{-/-}$ and *DKO* mice represents the impact of Tet2 loss on the genome of these cells. The small amount of overlap between DhMRs and DMRs within each genotype of LK cells is surprising, but these results suggest that decreased-5hmC does not necessarily result in increased-5mC in a specific locus of genome. It will be very informative to map in these cells, 5fC and 5caC genomic profiles simultaneously to determine their overlap with 5hmC or 5mC changes in the genome. As well, we observed no correlation between gene expression and DhMRs or DMRs in these LK cells that were isolated from pre-leukemic $Tet2^{-/-}$ or *DKO* mice. Similar observations have been reported in mouse ES cells (Ficz et al., 2011; Pastor et al., 2011; Williams et al., 2011). These observations suggest that distinct cytosine modifications (particularly 5hmC) mark specific genes in $Tet2^{-/-}$ or *DKO* LK cells without altering their expression. Such could work together with other genomic insults to alter gene expression. Indeed, the global transcriptome changed dramatically in transformed B-ALL *DKO* tumor cells, and most of these dysregulated genes are direct targets of Tet1 or Tet2. A recent study has shown that Tet2 loss cooperates with AML1-ETO oncogene to promote DNA hypermethylation on enhancers (leading to the loss of enhancer activity), resulting in lowered gene expression (Rasmussen et al., 2015), while Tet2 loss alone is likely unable to achieve this effect. Another recent study has shown that combined *Tet2* loss and *Flt3* mutation alter DNA methylation and gene expression in LSK cells, but not with either mutation alone, and similar results are seen in human AML patients with combined *TET2* and *FLT3* mutations (Shih et al., 2015).

These findings have several layers of implications: (1) they highlight the critical roles of each of the enzymes and the possible lines of communication between Tet1 and Tet2 in homeostasis of hematopoiesis and pathogenesis of hematological malignancies; (2) despite their similar catalytic activities in oxidization of 5mC, Tet1 is required for the *Tet2*-deletion-mediated HSC dysregulation, myeloid skewing, and myeloid malignancy development; TET1 therefore, likely plays a distinct role in myeloid leukemogenesis in the context of TET2 loss; (3) Tet1 and Tet2 seem to have overlapping roles in B cell development/tumorigenesis, where loss of Tet1 alone causes B cell malignancies and loss of both enzymes accelerates pathogenesis of B cell malignancies. This study expands upon our previous work that implicated Tet2 in myeloid malignancies (Li et al., 2011) and Tet1 in lymphoid malignancies (Cimmino et al., 2015). Our present studies suggest a novel role for Tet1 in Tet2-loss-mediated leukemogenesis as such making it a potential target for therapeutic intervention in myeloid malignancy patients. Moreover, it reveals that combined loss of Tet1/2 in mice induces B cell malignancies with a long latency. However, early changes in DNA 5hmC/5mC, CLP/BLP pool, and B cell development precede the development of disease. Whether Tet1/2 loss promotes changes in chromatin accessibility that facilitates acquisition of additional mutations requires further investigation. In summary, the studies presented here identify overlapping, non-redundant, and even opposite functions for Tet1 and Tet2 in hematopoietic regulation and leukemogenesis. Therefore, these studies provide a framework on pathology for further elucidating molecular mechanisms of critical lines of communication between TET1 and TET2 in the pathogenesis of hematological malignancies.

EXPERIMENTAL PROCEDURES

Generation of *Tet1* and *Tet2* Conditional Knockout Mice

Tet2:flox allele mice were generated as follows: the targeting vector was constructed in a plasmid containing a *Neo* cassette flanked by two *FRT* sites. A 0.8-kb genomic fragment containing the 11^{th} exon of *Tet2* (coding part of the catalytic domain) was inserted between two *loxP* sites (cassette map: *loxP-exon11-loxP-FRT-Neo-FRT*, Figure S4A). For gene targeting, 4.4-kb 5′ and 3.6-kb 3′ arm genomic fragments were subcloned into the vector. The targeting vector was electroporated into 129/sv ES cells and subsequently screened by Southern blot (Figure S4B). Two positive clones were selected for the blastocyst injection. Male chimeric mice were crossed to C57BL/6 females to screen for germline transmission of *Tet2:flox* allele ($Tet2^{f/+}$). $Tet2^{f/+}$ mice were crossed to *Flippase* deleter mice to remove the *Neo* cassette (Figure S4B) (Li et al., 2011; Wang et al., 2014). *Tet1:flox* allele mice were generated from the previously reported $Tet1^{+/H}$ mESCs (Dawlaty et al., 2011) as outlined in Figures S4C and S4D. $Tet2^{f/f}$;*MxCre*, $Tet1^{f/f}$;*MxCre* and $Tet1^{f/f}$; $Tet2^{f/f}$;*MxCre* mice were produced for studies. MxCre expression was induced

by intraperitoneal injection of three doses of 300 μg of polyinosine-polycytosine (*pI:pC*) (Figure S4E). Animal care was in accordance with institutional guidelines and approved by the Institutional Animal Care and Use Committee (IACUC), University of Miami Miller School of Medicine and Department of Comparative Medicine, and Massachusetts Institute of Technology.

Bioinformatics and Statistical Analyses

hME-Seal was performed as described previously (Song et al., 2011). MeDIP was performed according to the manufacturer's protocol. Bioinformatics analysis for 5hmC-seq and MeDIP-seq were described previously (Szulwach et al., 2011; Yao et al., 2014). Differences between experimental groups were determined by the Student's t test or ANOVA followed by Newman-Keuls multiple comparison tests as appropriate. p values <0.05 were considered significant.

ACCESSION NUMBERS

Sequence data have been deposited to the NCBI GEO and are available under accession number GEO: GSE73611.

SUPPLEMENTAL INFORMATION

Supplemental Information includes Supplemental Experimental Procedures, six figures, and eight tables and can be found with this article online at http://dx.doi.org/10.1016/j.celrep.2015.10.037.

AUTHOR CONTRIBUTIONS

Z.Z., M.M.D., F.P., J.W., and S.C. performed the experiments involving animal models; Z.Z., Y.Z., Z.C., H.S., and W.Y. performed experiments involving human specimens; H.N. reviewed the blood smears and histopathologic sections; L.C., L.L., Z.Q., and P.J. analyzed the RNA-seq/5mC/5hmC data. M.M.D., O.W., S.D.N., F.-C.Y., and R.J. participated in designing the study and revised the manuscript; P.J. and M.X. designed and supervised the studies, performed the experiments, analyzed data, wrote the manuscript, and are responsible for its final draft.

ACKNOWLEDGMENTS

This work was supported by grants from the NIH (HL112294 to M.X., CA172408 to M.X. and F.-C.Y., NS079625 and MH102690 to P.J., HDO45022 and CA084198 to R.J.), Simons Foundation (to R.J. and P.J.), and National Nature Science Foundation of China (#81328003 to W.Y.). M.M.D. is a Damon Runyon Postdoctoral Fellow.

Received: May 11, 2015
Revised: August 26, 2015
Accepted: October 11, 2015
Published: November 12, 2015

REFERENCES

Abdel-Wahab, O., Gao, J., Adli, M., Dey, A., Trimarchi, T., Chung, Y.R., Kuscu, C., Hricik, T., Ndiaye-Lobry, D., Lafave, L.M., et al. (2013). Deletion of Asxl1 results in myelodysplasia and severe developmental defects in vivo. J. Exp. Med. *210*, 2641–2659.

Bock, C., Beerman, I., Lien, W.H., Smith, Z.D., Gu, H., Boyle, P., Gnirke, A., Fuchs, E., Rossi, D.J., and Meissner, A. (2012). DNA methylation dynamics during in vivo differentiation of blood and skin stem cells. Mol. Cell *47*, 633–647.

Chambers, S.M., Boles, N.C., Lin, K.Y., Tierney, M.P., Bowman, T.V., Bradfute, S.B., Chen, A.J., Merchant, A.A., Sirin, O., Weksberg, D.C., et al. (2007). Hematopoietic fingerprints: an expression database of stem cells and their progeny. Cell Stem Cell *1*, 578–591.

Cimmino, L., Dawlaty, M.M., Ndiaye-Lobry, D., Yap, Y.S., Bakogianni, S., Yu, Y., Bhattacharyya, S., Shaknovich, R., Geng, H., Lobry, C., et al. (2015). TET1 is a tumor suppressor of hematopoietic malignancy. Nat. Immunol. *16*, 653–662.

Dawlaty, M.M., Ganz, K., Powell, B.E., Hu, Y.C., Markoulaki, S., Cheng, A.W., Gao, Q., Kim, J., Choi, S.W., Page, D.C., and Jaenisch, R. (2011). Tet1 is dispensable for maintaining pluripotency and its loss is compatible with embryonic and postnatal development. Cell Stem Cell *9*, 166–175.

Delhommeau, F., Dupont, S., Della Valle, V., James, C., Trannoy, S., Massé, A., Kosmider, O., Le Couedic, J.P., Robert, F., Alberdi, A., et al. (2009). Mutation in TET2 in myeloid cancers. N. Engl. J. Med. *360*, 2289–2301.

Deplus, R., Delatte, B., Schwinn, M.K., Defrance, M., Méndez, J., Murphy, N., Dawson, M.A., Volkmar, M., Putmans, P., Calonne, E., et al. (2013). TET2 and TET3 regulate GlcNAcylation and H3K4 methylation through OGT and SET1/COMPASS. EMBO J. *32*, 645–655.

Ficz, G., Branco, M.R., Seisenberger, S., Santos, F., Krueger, F., Hore, T.A., Marques, C.J., Andrews, S., and Reik, W. (2011). Dynamic regulation of 5-hydroxymethylcytosine in mouse ES cells and during differentiation. Nature *473*, 398–402.

He, Y.F., Li, B.Z., Li, Z., Liu, P., Wang, Y., Tang, Q., Ding, J., Jia, Y., Chen, Z., Li, L., et al. (2011). Tet-mediated formation of 5-carboxylcytosine and its excision by TDG in mammalian DNA. Science *333*, 1303–1307.

Huang, H., Jiang, X., Li, Z., Li, Y., Song, C.X., He, C., Sun, M., Chen, P., Gurbuxani, S., Wang, J., et al. (2013). TET1 plays an essential oncogenic role in MLL-rearranged leukemia. Proc. Natl. Acad. Sci. USA *110*, 11994–11999.

Ito, S., Shen, L., Dai, Q., Wu, S.C., Collins, L.B., Swenberg, J.A., He, C., and Zhang, Y. (2011). Tet proteins can convert 5-methylcytosine to 5-formylcytosine and 5-carboxylcytosine. Science *333*, 1300–1303.

Iyer, L.M., Tahiliani, M., Rao, A., and Aravind, L. (2009). Prediction of novel families of enzymes involved in oxidative and other complex modifications of bases in nucleic acids. Cell Cycle *8*, 1698–1710.

Jankowska, A.M., Szpurka, H., Tiu, R.V., Makishima, H., Afable, M., Huh, J., O'Keefe, C.L., Ganetzky, R., McDevitt, M.A., and Maciejewski, J.P. (2009). Loss of heterozygosity 4q24 and TET2 mutations associated with myelodysplastic/myeloproliferative neoplasms. Blood *113*, 6403–6410.

Ko, M., Bandukwala, H.S., An, J., Lamperti, E.D., Thompson, E.C., Hastie, R., Tsangaratou, A., Rajewsky, K., Koralov, S.B., and Rao, A. (2011). Ten-Eleven-Translocation 2 (TET2) negatively regulates homeostasis and differentiation of hematopoietic stem cells in mice. Proc. Natl. Acad. Sci. USA *108*, 14566–14571.

Langemeijer, S.M., Kuiper, R.P., Berends, M., Knops, R., Aslanyan, M.G., Massop, M., Stevens-Linders, E., van Hoogen, P., van Kessel, A.G., Raymakers, R.A., et al. (2009). Acquired mutations in TET2 are common in myelodysplastic syndromes. Nat. Genet. *41*, 838–842.

Li, Z., Cai, X., Cai, C.L., Wang, J., Zhang, W., Petersen, B.E., Yang, F.C., and Xu, M. (2011). Deletion of Tet2 in mice leads to dysregulated hematopoietic stem cells and subsequent development of myeloid malignancies. Blood *118*, 4509–4518.

Mallampati, S., Sun, B., Lu, Y., Ma, H., Gong, Y., Wang, D., Lee, J.S., Lin, K., and Sun, X. (2014). Integrated genetic approaches identify the molecular mechanisms of Sox4 in early B-cell development: intricate roles for RAG1/2 and CK1ε. Blood *123*, 4064–4076.

Moran-Crusio, K., Reavie, L., Shih, A., Abdel-Wahab, O., Ndiaye-Lobry, D., Lobry, C., Figueroa, M.E., Vasanthakumar, A., Patel, J., Zhao, X., et al. (2011). Tet2 loss leads to increased hematopoietic stem cell self-renewal and myeloid transformation. Cancer Cell *20*, 11–24.

Musialik, E., Bujko, M., Wypych, A., Matysiak, M., and Siedlecki, J.A. (2014). TET2 promoter DNA methylation and expression analysis in pediatric B-cell acute lymphoblastic leukemia. Hematol. Rep. *6*, 5333.

Natkunam, Y., Zhao, S., Mason, D.Y., Chen, J., Taidi, B., Jones, M., Hammer, A.S., Hamilton Dutoit, S., Lossos, I.S., and Levy, R. (2007). The oncoprotein LMO2 is expressed in normal germinal-center B cells and in human B-cell lymphomas. Blood *109*, 1636–1642.

Ono, R., Taki, T., Taketani, T., Taniwaki, M., Kobayashi, H., and Hayashi, Y. (2002). LCX, leukemia-associated protein with a CXXC domain, is fused

to MLL in acute myeloid leukemia with trilineage dysplasia having t(10;11)(q22;q23). Cancer Res. *62*, 4075–4080.

Ott, G., Rosenwald, A., and Campo, E. (2013). Understanding MYC-driven aggressive B-cell lymphomas: pathogenesis and classification. Blood *122*, 3884–3891.

Pastor, W.A., Pape, U.J., Huang, Y., Henderson, H.R., Lister, R., Ko, M., McLoughlin, E.M., Brudno, Y., Mahapatra, S., Kapranov, P., et al. (2011). Genome-wide mapping of 5-hydroxymethylcytosine in embryonic stem cells. Nature *473*, 394–397.

Pastor, W.A., Aravind, L., and Rao, A. (2013). TETonic shift: biological roles of TET proteins in DNA demethylation and transcription. Nat. Rev. Mol. Cell Biol. *14*, 341–356.

Pfeifer, M., Grau, M., Lenze, D., Wenzel, S.S., Wolf, A., Wollert-Wulf, B., Dietze, K., Nogai, H., Storek, B., Madle, H., et al. (2013). PTEN loss defines a PI3K/AKT pathway-dependent germinal center subtype of diffuse large B-cell lymphoma. Proc. Natl. Acad. Sci. USA *110*, 12420–12425.

Quivoron, C., Couronné, L., Della Valle, V., Lopez, C.K., Plo, I., Wagner-Ballon, O., Do Cruzeiro, M., Delhommeau, F., Arnulf, B., Stern, M.H., et al. (2011). TET2 inactivation results in pleiotropic hematopoietic abnormalities in mouse and is a recurrent event during human lymphomagenesis. Cancer Cell *20*, 25–38.

Rasmussen, K.D., Jia, G., Johansen, J.V., Pedersen, M.T., Rapin, N., Bagger, F.O., Porse, B.T., Bernard, O.A., Christensen, J., and Helin, K. (2015). Loss of TET2 in hematopoietic cells leads to DNA hypermethylation of active enhancers and induction of leukemogenesis. Genes Dev. *29*, 910–922.

Sakata-Yanagimoto, M., Enami, T., Yoshida, K., Shiraishi, Y., Ishii, R., Miyake, Y., Muto, H., Tsuyama, N., Sato-Otsubo, A., Okuno, Y., et al. (2014). Somatic RHOA mutation in angioimmunoblastic T cell lymphoma. Nat. Genet. *46*, 171–175.

Shih, A.H., Jiang, Y., Meydan, C., Shank, K., Pandey, S., Barreyro, L., Antony-Debre, I., Viale, A., Socci, N., Sun, Y., et al. (2015). Mutational cooperativity linked to combinatorial epigenetic gain of function in acute myeloid leukemia. Cancer Cell *27*, 502–515.

Shlush, L.I., Zandi, S., Mitchell, A., Chen, W.C., Brandwein, J.M., Gupta, V., Kennedy, J.A., Schimmer, A.D., Schuh, A.C., Yee, K.W., et al.; HALT Pan-Leukemia Gene Panel Consortium (2014). Identification of pre-leukaemic haematopoietic stem cells in acute leukaemia. Nature *506*, 328–333.

Simonetti, G., Carette, A., Silva, K., Wang, H., De Silva, N.S., Heise, N., Siebel, C.W., Shlomchik, M.J., and Klein, U. (2013). IRF4 controls the positioning of mature B cells in the lymphoid microenvironments by regulating NOTCH2 expression and activity. J. Exp. Med. *210*, 2887–2902.

Song, C.X., Szulwach, K.E., Fu, Y., Dai, Q., Yi, C., Li, X., Li, Y., Chen, C.H., Zhang, W., Jian, X., et al. (2011). Selective chemical labeling reveals the genome-wide distribution of 5-hydroxymethylcytosine. Nat. Biotechnol. *29*, 68–72.

Sun, D., Luo, M., Jeong, M., Rodriguez, B., Xia, Z., Hannah, R., Wang, H., Le, T., Faull, K.F., Chen, R., et al. (2014). Epigenomic profiling of young and aged HSCs reveals concerted changes during aging that reinforce self-renewal. Cell Stem Cell *14*, 673–688.

Szulwach, K.E., Li, X., Li, Y., Song, C.X., Wu, H., Dai, Q., Irier, H., Upadhyay, A.K., Gearing, M., Levey, A.I., et al. (2011). 5-hmC-mediated epigenetic dynamics during postnatal neurodevelopment and aging. Nat. Neurosci. *14*, 1607–1616.

Tahiliani, M., Koh, K.P., Shen, Y., Pastor, W.A., Bandukwala, H., Brudno, Y., Agarwal, S., Iyer, L.M., Liu, D.R., Aravind, L., and Rao, A. (2009). Conversion of 5-methylcytosine to 5-hydroxymethylcytosine in mammalian DNA by MLL partner TET1. Science *324*, 930–935.

Wang, J., Li, Z., He, Y., Pan, F., Chen, S., Rhodes, S., Nguyen, L., Yuan, J., Jiang, L., Yang, X., et al. (2014). Loss of Asxl1 leads to myelodysplastic syndrome-like disease in mice. Blood *123*, 541–553.

Williams, K., Christensen, J., Pedersen, M.T., Johansen, J.V., Cloos, P.A., Rappsilber, J., and Helin, K. (2011). TET1 and hydroxymethylcytosine in transcription and DNA methylation fidelity. Nature *473*, 343–348.

Yao, B., Lin, L., Street, R.C., Zalewski, Z.A., Galloway, J.N., Wu, H., Nelson, D.L., and Jin, P. (2014). Genome-wide alteration of 5-hydroxymethylcytosine in a mouse model of fragile X-associated tremor/ataxia syndrome. Hum. Mol. Genet. *23*, 1095–1107.

Yoshimatsu, Y., Yamazaki, T., Mihira, H., Itoh, T., Suehiro, J., Yuki, K., Harada, K., Morikawa, M., Iwata, C., Minami, T., et al. (2011). Ets family members induce lymphangiogenesis through physical and functional interaction with Prox1. J. Cell Sci. *124*, 2753–2762.